Published online 18 October 2011 *Nucleic Acids Research, 2012, Vol. 40, No. 3* ***1191–1202***
doi:10.1093/nar/gkr858

Characterization of the 6-methyl isoxanthopterin (6-MI) base analog dimer, a spectroscopic probe for monitoring guanine base conformations at specific sites in nucleic acids

Kausiki Datta[1,2], Neil P. Johnson[3,4,5], Giuseppe Villani[3,4], Andrew H. Marcus[5] and Peter H. von Hippel[1,*]

[1]Department of Chemistry and Institute of Molecular Biology, University of Oregon, Eugene, OR 97403, USA, [2]Hoffmann-La Roche, Nutley, NJ 07110, USA [3]CNRS IPBS (Institut de Pharmacologie et de Biologie Structurale), F-31077, Toulouse, France, [4]Université de Toulouse, UPS, IPBS, F-31077, Toulouse, France and [5]Department of Chemistry, Oregon Center for Optics, Institute of Molecular Biology, University of Oregon, Eugene, OR 97403, USA

Received August 8, 2011; Revised September 23, 2011; Accepted September 26, 2011

ABSTRACT

We here characterize local conformations of site-specifically placed pairs of guanine (G) residues in RNA and DNA, using 6-methyl isoxanthopterin (6-MI) as a conformational probe. 6-MI is a base analog of G and spectroscopic signals obtained from pairs of adjacent 6-MI residues reflect base–base interactions that are sensitive to the sequence context, local DNA conformation and solvent environment of the probe bases. CD signals show strong exciton coupling between stacked 6-MI bases in double-stranded (ds) DNA; this coupling is reduced in single-stranded (ss) DNA sequences. Solvent interactions reduce the fluorescence of the dimer probe more efficiently in ssDNA than dsDNA, while self-quenching between 6-MI bases is enhanced in dsDNA. 6-MI dimer probes closely resemble adjacent GG residues, in that these probes have minimal effects on the stability of dsDNA and on interactions with solvent additive betaine. They also serve as effective template bases, although further polymerase-dependent extension of DNA primers past 6-MI template bases is significantly inhibited. These probes are also used to monitor DNA 'breathing' at model replication forks. The 6-MI dimer probe can serve in many contexts as a useful tool to investigate GG conformations at specific sites within the nucleic acid frameworks of functioning macromolecular machines in solution.

INTRODUCTION

Defined conformational changes of nucleic acids at specific sites within protein–nucleic acid complexes are central to the mechanisms by which the macromolecular machines of gene-expression process and manipulate DNA and RNA. The UV absorbance and circular dichroism (CD) signals of individual base residues are masked by contributions from all the nucleotide and amino acid residues present within the complex. This limitation can be overcome by substituting specific nucleic acid bases with analogs that absorb light at wavelengths >300 nm, where proteins and canonical nucleic acid bases are transparent. Examples include the adenine (A) analog 2-aminopurine (2-AP, A_{max} at 310 nm) and the cytosine (C) analog pyrrolocytosine (PC, A_{max} at 350 nm).

Nucleic acids labeled with these base analogs exhibit CD signals at long wavelengths (which we call low energy CD) that can provide information about local conformations of the probe residues (1,2). For example, CD spectra exhibit strong exciton coupling between adjacent probe residues, which is characteristic of B-form duplex DNA (1–8). The fluorescence spectra of these residues give additional information about the site-specific behavior of the nucleic acid components, although we note base analogs that give low energy CD spectra need not be fluorescent (9). We have used these approaches to study nucleic

*To whom correspondence should be addressed. Tel: +1 541 346 5151; Fax: +1 541 346 5891; Email: petevh@molbio.uoregon.edu

The authors wish it to be known that, in their opinion, the first two authors should be regarded as joint First Authors.

acid conformation changes within large macromolecular complexes involved in replication and transcription (3,5–8,10).

Here we characterize the guanine analog, 6-methyl isoxanthopterin (6-MI, A_{max} at 350 nm) as a dimer probe of local DNA conformation. 6-MI (Figure 1) is a fluorescent base analog that has previously been incorporated as a monomer probe to study the local environments of specific guanine (G) residues in DNA (11–15). The presence of a single 6-MI residue in double-stranded (ds) DNA has little effect on the stability of the DNA duplex, suggesting that this probe accurately reflects the structure and chemistry of G residues within dsDNA. The 6-MI base is fluorescent, with an emission peak ~450 nm. In comparison to single-stranded (ss) DNA of the same sequence, the fluorescence signal in dsDNA is generally significantly quenched by base-stacking interactions. The responsiveness of the fluorescence signal of 6-MI to base-stacking and DNA sequence context makes this an attractive base analog to use in investigations of conformational changes at specific positions within GC-rich nucleic acid sequences.

Dimer probes can provide local structural information that is not available with single (monomer) probes. In particular, dimer probes can undergo exciton coupling between the two residues of the probe, and in favorable cases the resulting CD spectra provide explicit information about the relative conformation of the two residues (1,2). We recently used the 6-MI dimer probe to investigate local conformational changes in primer–template (P/T) DNA during DNA replication by the Klenow Fragment of DNA polymerase I (KF DNAP) (3). Structural studies of A-family DNA polymerases, such as KF DNAP, show that the coding base on the template strand has a characteristic 'flipped-out' extra-helical conformation that occupies a 'pre-insertion site' within the polymerase in the binary complex (protein and nucleic acid framework) (16–18). Addition of the correct nucleoside triphosphate (dNTP) induces a closed ternary complex in which the template base re-stacks within the DNA helix to form a base pair (bp) with the incoming dNTP (16,18). CD spectra of a 6-MI dimer probe at the template–base position clearly showed these rearrangements in a functioning polymerase in solution (3). Local DNA conformations that appear to be associated with initial steps of dNTP selection (19–22) were also observed.

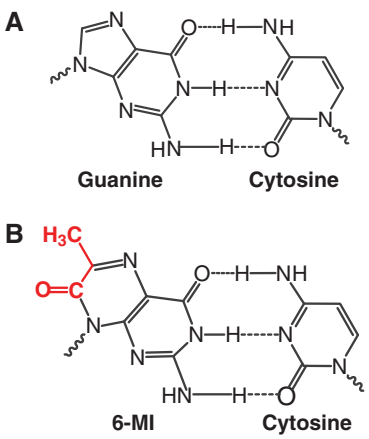

Figure 1. Base pair structures. G•C **(A)** and probable 6-MI•C **(B)** base pair structures. The chemical features of 6-MI that differ from G are highlighted in red.

In order to provide a background for further applications, we have investigated the potential and limitations of the 6-MI dimer as a probe of local DNA conformation. The absorbance, fluorescence and CD spectra of 6-MI dimers were measured in ss and dsDNA environments, as well as in various positions at and near P/T DNA junctions. Sequence effects on these spectroscopic properties were examined. We also determined the effect of 6-MI dimer probes on the stability of duplex DNA. In addition, the effect of the dimer probe on the accessibility of the DNA structure to small binding ligands was investigated by measuring the effect of the amino acid analog betaine on both the general and the base-pair-specific thermal stability of duplex DNAs. Finally we analyzed the effects of the 6-MI dimer probe on DNA coding and templating properties in replication. Taken together these results suggest that 6-MI dimer probes can serve as a rich source of information about site-specific conformations of nucleic acid bases within DNA constructs, both free in solution and within macromolecular complexes.

MATERIALS AND METHODS

Unlabeled and 6-MI-labeled DNA oligonucleotides were purchased from Integrated DNA Technologies (Coralville, IA) and from Fidelity Systems (Gaithersburg, MD). DNA sequences and nomenclature are shown in the figures. Oligonucleotide concentrations were determined using extinction coefficients furnished by the manufacturer. Duplex constructs were made by heating equimolar concentrations of complementary strands to 90°C, followed by gradual cooling.

Fluorescence spectra were measured with Jobin–Yvon Fluorolog and Photon Technology International spectrometers. Unless otherwise stated, samples were excited at 350 nm and emission spectra recorded from 340 to 500 nm. CD spectra of 3 μM concentrations of oligonucleotide were measured using a Jasco model J-720 CD spectrophotometer equipped with a temperature-controlled cell holder, as previously described (3). CD values reported represent the average of 8–10 independent measurements in units of ε_L–ε_R (in $M^{-1}cm^{-1}$), and were reported per mole of 6-MI residue for 6-MI dimer probes in low-energy CD spectra at 300–450 nm, or per mole of nucleotide in CD spectra measured at 230–300 nm.

In DNA melting experiments the UV absorbance of 1 μM DNA was monitored at either 260 nm ($A_{260\,nm}$) or 350 nm ($A_{350\,nm}$), using a Cary UV spectrophotometer equipped with a Peltier temperature controller. Samples were heated at 1°C min^{-1}) from 7°C to 90°C and the absorption was measured at every 1°C step. Thermal melting of 6-MI-labeled duplex DNA was also monitored by

fluorescence at 430 nm, using the same DNA concentrations and buffer conditions as for the UV absorbance studies. Melting curves represent averaged data for three freshly prepared DNA constructs. Melting temperature (T_m) values were determined using a modified van't Hoff equation that simultaneously fits the native and denatured state baselines and the transition region (23). When present, the concentration of betaine used as a small molecule solvent additive was 5.5 M.

DNA replication studies were performed using two protocols. (i) KF *exo-* DNA polymerase was purified as previously described (24) and polymerase activity was measured in buffer containing 20 mM HEPES (pH 7.9), 100 mM sodium acetate, 10 mM $Mg(OAc)_2$ and 1 mM DTT, using 3 μM concentrations of P/T DNA and 500 μM dNTPs, and incubated at 25°C for time periods up to 1 h. (ii) KF DNAP was purchased from New England BioLabs and assays were performed at 37°C for the time periods indicated in reaction mixtures containing 10 mM Tris–HCl (pH 7.9), 10 mM $MgCl_2$, 50 mM NaCl, 1 mM DTT and quantities of DNA template, KF DNAP and dNTPs specified for each experiment. In both cases primer strands were labeled at the 5′-terminus with γ–P^{32}-ATP and DNA products were separated on 12–15% sequencing gels in 7 M urea and then visualized and quantified using the Molecular Dynamics PhosphorImager with ImageQuant software.

RESULTS

Interactions between the 6-MI bases of the dimer probe induce changes in spectroscopic signals

6-MI-modified DNA displays an absorption peak at 345–350 nm, a wavelength region that is transparent for protein components and canonical DNA bases. Dimer probes display absorption maxima at *higher* energies for the same ssDNA sequence, relative to the monomer (Figure 2A), although the extent of this blue shift can depend on the identity of the adjacent canonical bases (Supplementary Table S1). As expected, hypochromism is observed in the spectrum of the 6-MI residue in dsDNA (Figure 2C and Table 1). Duplex DNA sequences containing dimer probes also absorb at *higher* energies than do dsDNA molecules containing a single 6-MI base in the same sequence context (Figure 2B). However, UV spectra of both monomer- and dimer-modified dsDNA are displaced toward *lower* energies relative to their corresponding ssDNA spectra.

If interactions between the 6-MI bases of the dimer probe are responsible for the observed blue shift, then separating the bases should reduce this effect. To test this suggestion the dimer probe was placed within the loop of a stem–loop construct in which—judging from the hyperchromism of the signal—6-MI bases are more unstacked than in ssDNA (Figure 2D). The UV spectrum shifted toward the red as expected. Consistent with this result, a spectral shift was not observed for ssDNA oligonucleotide containing a TgTgG sequence (g indicates a 6-MI residue), suggesting that separation of the

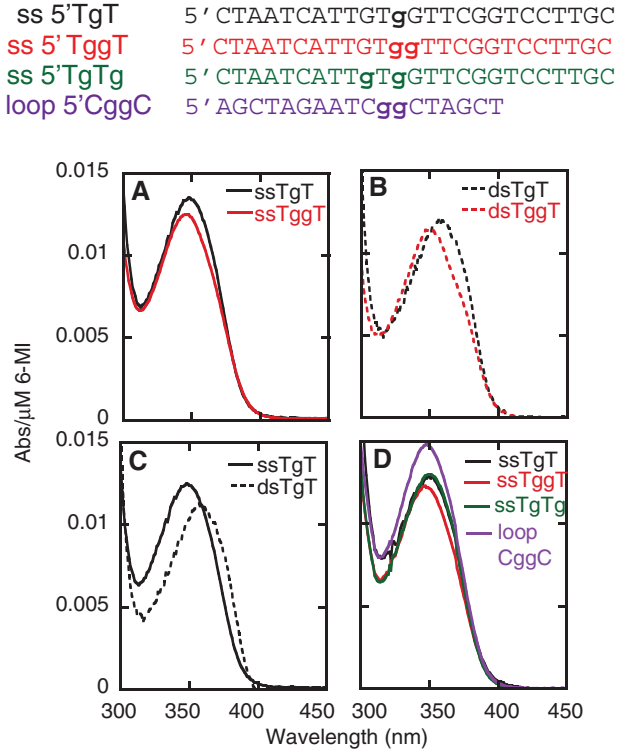

Figure 2. UV absorption spectra of 6-MI monomer and dimer in various DNA constructs. Sequences and their designations are shown at the top. 6-MI is represented as 'g'. Solid lines are ssDNA molecules and dotted lines are duplexes of the indicated ssDNA construct with a fully complementary strand. The spectra of TgT-containing constructs are shown in black; those for TggT in red; those for TgTgG in green; and those for g-containing stem–loop constructs in purple.

6-MI residues in ssDNA by an intervening base uncouples the electronic transitions of the 6-MI residues.

To our knowledge the extinction coefficient of 6-MI has not been reported. We note that this parameter can be estimated from Figure 2 as $\varepsilon_{350} \sim 12\,000\,M^{-1}cm^{-1}$. In our experiments in this article, 6-MI concentrations were calculated from oligonucleotide concentrations (as determined by A_{260} values and the manufacturer's extinction coefficient) and from the number of probe residues, with no corrections for effects of DNA sequence or secondary structure.

In contrast to UV absorption, fluorescence emission of monomer and dimer 6-MI probes in otherwise identical ssDNA occurred at the same wavelength (Figure 3B), although the fluorescence intensity per mole of 6-MI was dramatically reduced in the dimer construct. Unlike UV absorption, the position of the fluorescence emission maximum was generally displaced towards higher energies in dsDNA constructs relative to the equivalent ssDNA strands (Figure 3A and Table 1). We note also that varying the excitation wavelength from 320 to 370 nm increased the wavelength of maximum fluorescence emission of dimer probes in duplex DNA from 418 to 430 nm (Supplementary Figure S1). Formation of dsDNA also quenched the fluorescence intensity of the 6-MI probe in all sequences except GggG. In contrast to previously reported results (14), we observed that the

Table 1. UV absorption and fluorescence spectral changes of 6-MI modified ss and dsDNA in various sequence contexts*

DNA seq.	UV ABSORPTION		FLUORESCENCE (Δ_{ex} 350 nm)		
	Δλ abs.	Rel. max intensity abs.	Δλ Fl	Rel. max intensity Fl.	
TgT ss	0	1	0	1	Figures 2 and 3
ds	10	0.90	0	0.63	
TggT ss	0	1	0	1	Figures 2 and 3
ds	3	0.94	−3	0.36	
P/T (*n*,*n*+1)	0	0.96	−1	1.47	
TgTgG ss	0	1	0	1	Figure 2
ds	6	0.91	0	0.55	
P/T (*n*+1,*n*+3)	1	0.90	−2	1.84	
TgG ss	0	1	0	1	–
ds	6	0.98	−7	0.36	
P/T (*n*)	0	0.95	−2	2.09	
CggT ss	0	1	0		
ds	5	0.96	−5	0.31	Figures 3 and 5
AXXT ss	–	–	0	1	Figure 4
ds	–	–	−6	0.1	
P/T (*n*,*n*+1)	–	–	−2	1.8	
GgG ss	0	1	1	1	–
ds	1	0.84	−9	0.44	
GggG ss	0	1	1	1	
ds	0	0.86	−9	1.86	–

*The Rel. max intensities correspond to the maximum intensity with respect to the signal of the equivalent ssDNA construct for each case. Δλ represents {wavelength of maximum intensity dsDNA [nm] -wavelength maximum intensity ssDNA [nm]}. Sequences are shown in the indicated figures. TgG occurs in 5′-C TAA TCA TTX TgG TTC GGT CCT TGC; GgG in 5′-C TAA TCA TTG gG TTC GGT CCT TGC; and GggG in 5′- C TAA TCA TTG ggG TTC GGT CCT TGC. dsDNA indicates duplex DNA with the complementary sequence; P/T is a Primer–Template DNA construct, symbols in parentheses designate the position of the 3′-primer terminus (Figure 4).

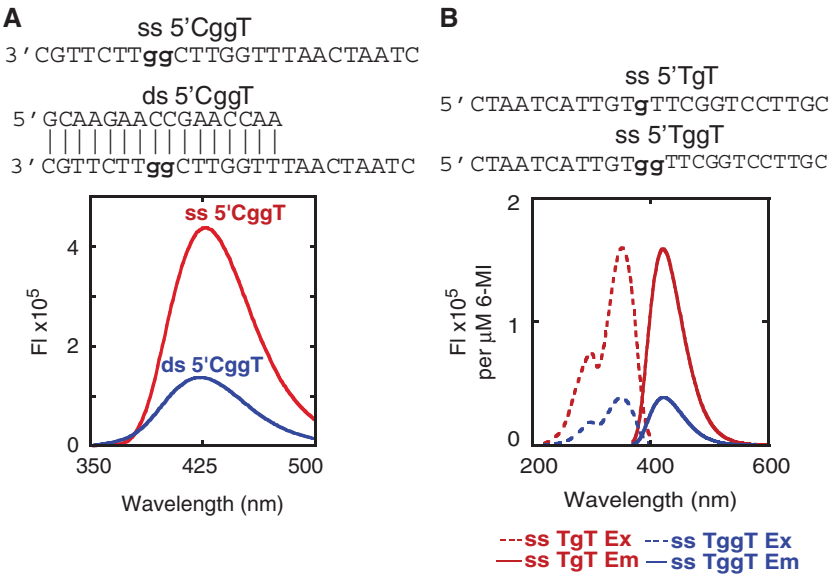

Figure 3. Fluorescence of 6-MI dimer. **(A)** Fluorescence of 6-MI probe dimers in ss and dsDNA. **(B)** Excitation (dashed line) and emission (solid line) spectra of ssDNA construct with a 6-MI monomer (red) and or a dimer (blue) probe. The sequence and nomenclature of the constructs are shown at the top. 'g' indicates 6-MI.

fluorescence of a single 6-MI base flanked by T residues *decreased* in dsDNA (Table 1).

Replacing the flanking T bases of the sequences in Figure 3B by G bases reduced the fluorescence intensities obtained by a factor of 10, without a change in the general shapes and relative intensities of the excitation and emission spectra. The replacement of adjacent T bases with A has been reported to similarly reduce the fluorescence of 6-MI monomer residues (14). These effects may reflect the known capacity of adjacent purine bases to quench fluorescent probes as a result of enhanced stacking interactions with the fluorophore (25,26) and might also contribute to the self-quenching observed for the dimer probe (see 'Discussion' section).

Finally, as previously reported (3), coupling between adjacent 6-MI bases was also evident in the CD spectra of the 6-MI dimer probe at 300–450 nm. The low-energy CD of ssDNA displayed a small peak at 385 nm and a significant trough at 345 nm (dark green trace, Figure 4D). The amplitude of this CD peak increased dramatically upon annealing with a complementary ssDNA strand, together with a concomitant increase in the depth of the trough (red trace). This spectrum corresponds to the characteristic exciton-coupling signal of pairs of 6-MI bases in a right-handed helical B-form duplex conformation.

To illustrate how these spectroscopic signals can be used to study conformations of bases at defined positions within DNA molecules, we monitored behavior of the 6-MI dimer probe at various positions within a P/T DNA construct. CD spectra for the 6-MI probe residues in the duplex region exhibited an intense exciton signal that *decreased* in the ssDNA regions of the construct (Figure 4D). In contrast, the fluorescence signal for 6-MI dimers was *quenched* in the DNA duplex regions and *increased* in the ssDNA sequences (Figure 4C). The 6-MI fluorescence intensity corresponding to positions (*n,n+1*) was significantly enhanced, suggesting a highly unstacked conformation immediately adjacent to the ss–dsDNA junction, as previously observed using a 2-AP dimer probe (4). This fluorescence increase was observed for monomer or dimer 6-MI probes at this position within P/T DNA constructs in a variety of sequence contexts (Table 1). The fluorescence intensity enhancement occurred without shifting the wavelength of the emission maximum compared to ssDNA, consistent with a similar solvent relaxation of probe bases in these two contexts (see 'Discussion' section). In contrast, the CD spectrum of the 6-MI dimer probe at the *n,n+1* position was similar to that seen in ssDNA. We note that the change in low-energy CD of 2-AP dimer probes at *n,n+1* positions was also very small compared to the observed change in fluorescence intensity (4). In both cases the CD exhibited no evidence for exciton coupling, consistent with the absence of B-form stacking of the adjacent 6-MI residues at this site (Figure 4).

Probing the major groove of 6-MI-modified DNA

Betaine is an amino acid analog and small molecule solvent additive that has a general destabilizing effect on dsDNA. In addition, this solvent additive has a *differential* effect on the stability of A•T and G•C bp within duplex DNA, and as a result the T_m values of DNA molecules of all bp compositions shift to a single (common) temperature at 'isostabilizing' (~5.5 M) concentrations of betaine. This differential base-pair-specific melting temperature perturbation is thought to reflect, at least in part, the relatively stronger binding of betaine molecules at A•T relative to G•C bp in the major groove of B-form DNA (27,28). These betaine-induced effects on the stability of DNA bp occur without significant perturbation of the B-form structure or the electrostatic properties of the dsDNA, suggesting that the observed effects of betaine on the T_m of dsDNA molecules could provide some information about possible effects of 6-MI dimer probes on local dsDNA conformations, particularly in the vicinity of the major groove.

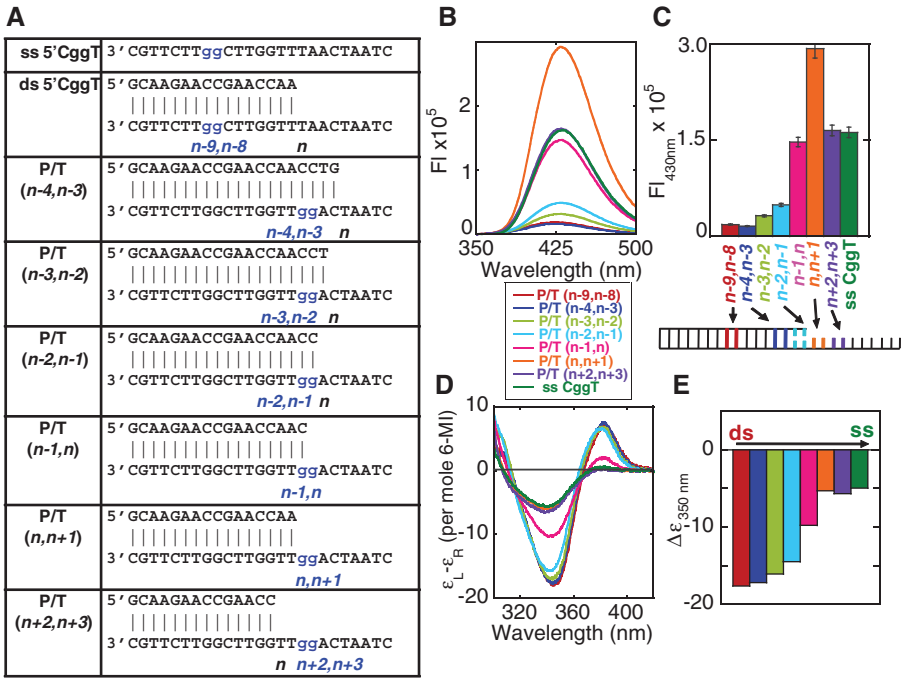

Figure 4. Spectroscopic signals of 6-MI dimer at various positions in P/T DNA. **(A)** Sequence and nomenclature of the constructs; 'gg' is 6-MI dimer. The template coding position is indicated as n, while the positions upstream and downstream are assigned negative (*n–1*, etc.) and positive (*n+1*, etc.) position numbers, respectively. **(B)** Fluorescence spectra. **(C)** Fluorescence intensity at 430 nm. **(D)** Low energy CD spectra. **(E)** CD intensity at 350 nm.

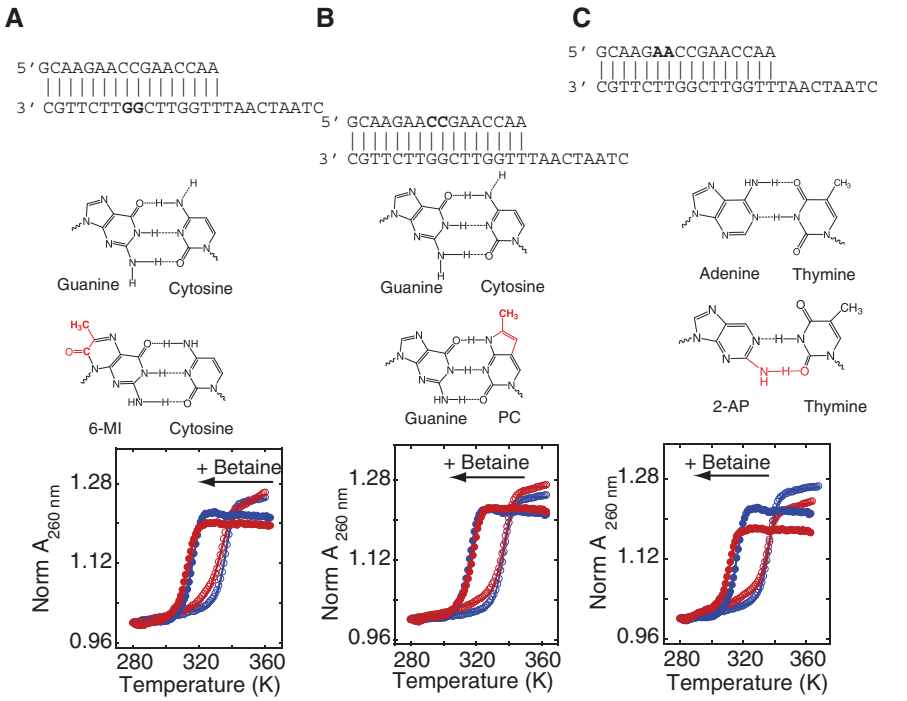

	No Betaine		Plus 5.5 M Betaine	
	T_m(°C)	ΔT_m(°C)(w.r.t. unlab construct)	T_m(°C)	ΔT_m(°C)(w.r.t. unlab construct)
Unmodified P/T DNA	63.4(±0.1)	0	42.9 (±0.1)	0
P/T DNA with 6-MI	59.9 (±0.3)	+3.5	39.9 (±0.1)	+3.0
P/T DNA with PC	64.2 (±0.2)	-0.8	44.8(±0.1)	-1.9
P/T DNA with 2-AP	61.5 (±0.2)	+1.9	38.7 (±0.1)	+4.2

Figure 5. Effect of dimer modifications on the thermal stability of dsDNA. UV absorbance at 260 nm of unmodified P/T DNA and P/T DNA containing 6-MI **(A)**; PC **(B);** or 2-AP **(C)** dimer probes in the absence and presence of betaine, as a function of temperature. Bold letters in the DNA sequences above each panel indicate the position of the modifications. Structures of 6-MI•C, PC•G, 2-AP•T and canonical base pairs are shown below the respective sequences. Absorbance thermal melting profiles of unmodified DNA constructs are shown in blue, and of dimer-containing DNA constructs in red. Open circles represent measurements made in the absence of betaine, while closed circles represent measurements made in solutions containing 5.5 M betaine. T_m values obtained from the melting profiles are listed in the table.

As expected from its effects on canonical DNAs, the addition of 5.5 M betaine to the solvent sharpened the melting transition of dsDNA as monitored by $A_{260\,nm}$, and dramatically reduced the observed T_m values for all duplex DNA molecules examined (Figure 5). In the absence of betaine the unmodified dsDNA construct showed a T_m value of 63.4°C, while the addition of 5.5 M betaine reduced the observed T_m to 42.9°C. The destabilizing effect of the 6-MI dimer probe on the T_m of the construct (∼−3.0°C) was unchanged by the addition of betaine.

Control experiments were carried out with two additional spectral probes that could also potentially alter interactions with betaine. The duplex portions of otherwise identical P/T DNA constructs were substituted with either 2-AP or PC dimers, replacing pairs of A or C residues, respectively. In the absence of betaine the PC dimer substitution *stabilized* the dsDNA (ΔT_m = +0.8°C) and betaine *increased* this effect (ΔT_m = +1.9°C). Insertion of the 2-AP dimer *destabilized* the duplex relative to the unmodified construct (ΔT_m = −1.9°C) and betaine further enhanced this destabilizing effect (to ΔT_m = –4.2°C). In all cases the T_m values obtained from local melting profiles agreed with the results obtained from global melting (Supplementary Figure S2), suggesting that betaine does not specifically perturb the stability or conformation of dsDNA sequences that contain this dimer probe. These results further suggest, as expected, that 6-MI dimer probes perturb major groove interactions less than do 2-AP or PC dimers, given that 2-AP and PC alter functional groups directly within the major groove while 6-MI does not.

6-MI dimer probes as template for DNA replication

KF DNA polymerase showed a strong preference for incorporating dCTP residues opposite a 6-MI dimer probe, as expected for template-directed synthesis with a G base analog (3) (Supplementary Figure S3). In addition 6-MI dimers probes placed in the template strand at

positions >3-bp *upstream* of the P/T junction had no effect on replication efficiency relative to the unmodified construct (Figure 6). However, dimer probes located 3 bp or less upstream from the P/T junction slightly *decreased* replication efficiency, while if located directly at the P/T junction or further downstream they significantly reduced the formation of full-length products. The appearance of shorter products reflects slowing or stalling of the polymerase *after* the incorporation of nucleotide residues opposite 6-MI.

To further explore the effects of a 6-MI dimer in the template strand we compared its behavior with the coding properties of a single 6-MI residue. We found that initial primer usage was identical for templates containing 6-MI or G (Figure 7B and Supplementary Figure S4) in the presence of all four canonical dNTPs. In addition the kinetics of the disappearance of the 13-mer primer bands in replication assays were the same (within experimental uncertainty) for the two templates, showing that a 6-MI coding base allows incorporation of the first dNTP as efficiently as a G coding base. However, after the addition of the first residue, the 6-MI-modified construct was poorly extended under conditions for which full-length product was observed in elongation reactions with the unmodified P/T substrate. Likewise, in the presence of dCTP and dATP (the dNTPs complementary to the first two coding bases), the unmodified P/T DNA substrate incorporated more than one dNTP with much higher frequency than modified DNA (Supplementary Figure S5). These results suggest that only the *extension* of the primer strand of a P/T DNA construct with a C•6-MI bp at the junction (and 6-MI in the template strand) is inhibited by the presence of the 6-MI base analog.

The capacity of a single 6-MI residue to code for each dNTP was measured as a function of DNA polymerase concentration (Figure 7C). As expected, incorporation of dCTP was the same for both templates (Figure 7B and Supplementary Figure S4). The relative incorporation of individual dNTPs across from both G and 6-MI template bases was the same, dCTP >> dATP > dGTP = dTTP, showing that G and 6-MI discriminate similarly against non-complementary dNTPs. The misincorporation frequency, however, was 3–5 times *lower* for the 6-MI coding base than for G (Supplementary Table S2). Misincorporation across from the 6-MI dimer was also less efficient than in unmodified templates (Supplementary Figure S3). The implications of these results for replication through base-analog-containing sequences are considered below.

DISCUSSION

Interactions between the bases of the 6-MI dimer probe

A variety of changes in the spectroscopic signals of the 6-MI dimer probe can potentially reveal information

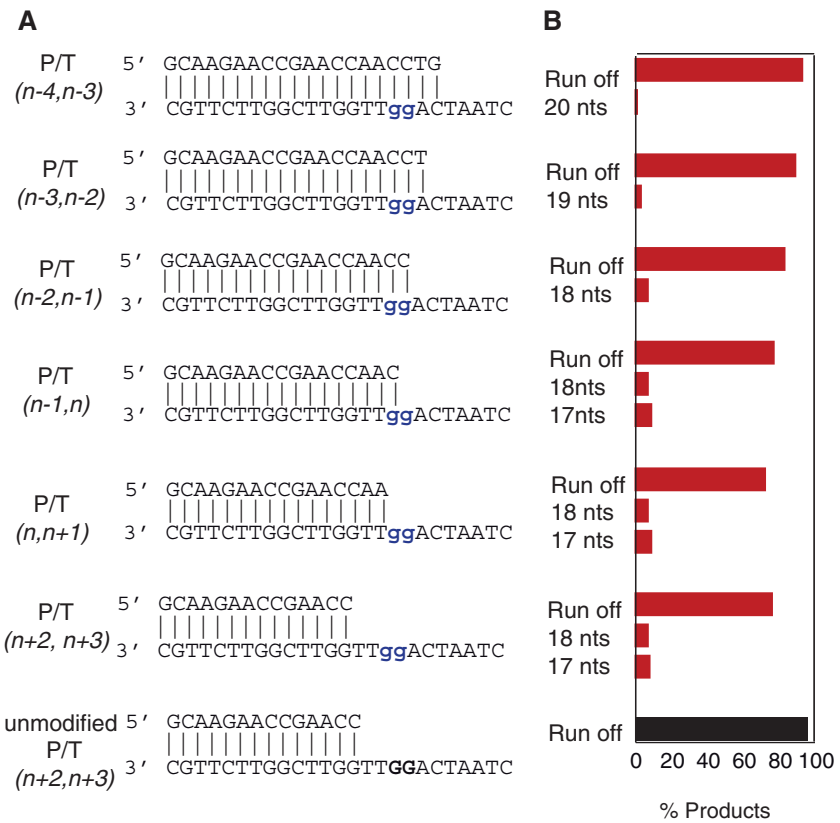

Figure 6. Replication of P/T DNA with a 6-MI dimer probe at various positions in the template strand. (A) The nomenclature and sequence of the P/T DNA constructs used. 'gg' shows the position of the dimer in the DNA constructs. (B) Histogram showing the percentage and the length of primer extension products formed for 6-MI modified (red) or unmodified (black) template after replication by KF. The polymerase activity was monitored at 25°C for 1 h using protocol (i), see text.

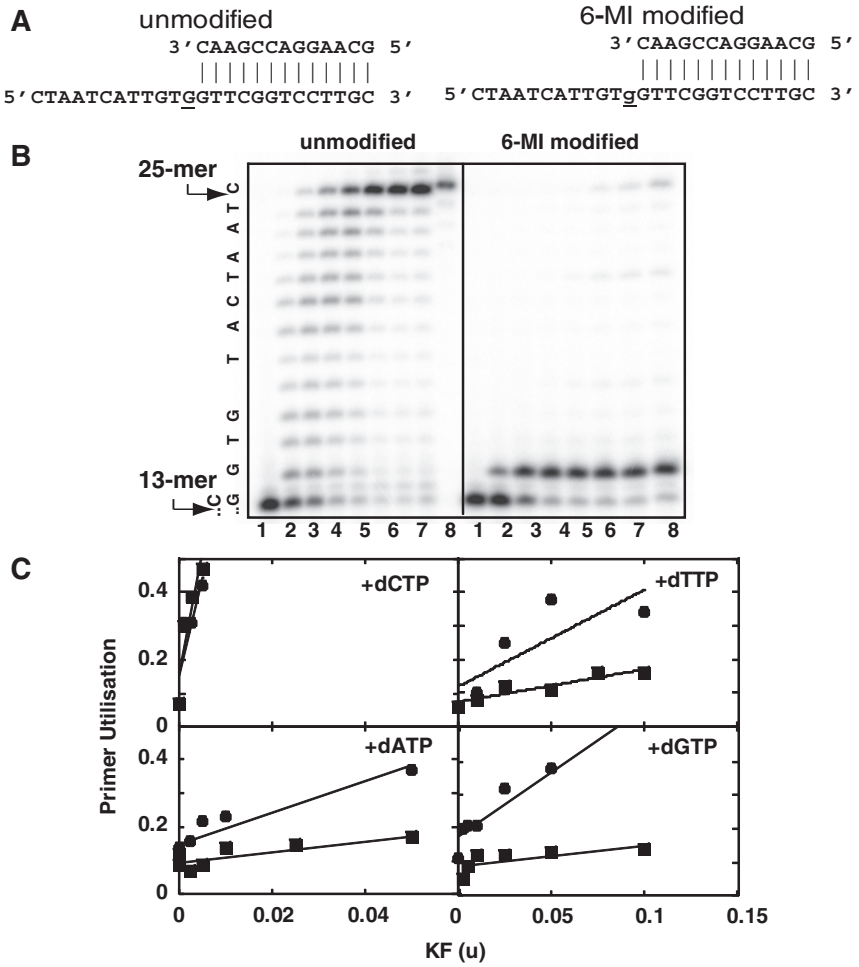

Figure 7. Replication of P/T DNA with a single 6-MI at the template coding position. (**A**) Sequences used; 6-MI is designated as 'g', the coding base is underlined. (**B**) Primer usage as a function of time. The 61 nM unmodified (left) or 6-MI-modified concentrations (right). P/T constructs were incubated with 0.05 nM KF in the presence of 35 μM concentrations of the four canonical dNTPs at 37°C for various times: 0.25 min (lane 2); 0.5 min (lane 3); 0.75 min (lane 4); 1 min (lane 5); 1.5 min (lane 6); 2 min (lane 7); 4 min (lane 8); and primer alone (lane 1). (**C**) Single nucleotide incorporation across from G or a single 6-MI coding base in the template DNA. The 61 nM concentrations of unmodified (circles) or 6-MI modified (squares) DNA constructs were incubated with increasing concentrations of KF for 10 min at 37°C in the presence of 350 μM of dCTP, dTTP, dATP or dGTP, as indicated. Replication was measured using protocol (ii). Primer utilization was calculated as {*1- [the intensity of the gel band of the primer strand]/[the intensity of the gel bands corresponding to the primer plus longer products]*}.

about changes in the conformations and environment of the probe bases. The dimer probe in both ds and ssDNA absorbs at higher energies than does the corresponding monomer probe (Figure 2). This blue shift seems to arise from base–base interactions within the dimer probe. Separating the 6-MI residues by an intervening base eliminates this effect, while placing probe residues into the loop of a stem–loop construct decreases the effect, presumably as a consequence of partial unstacking of the vicinal bases induced by the bending of the intervening sugar–phosphate backbone. These observations suggest that 6-MI bases couple via a side-by-side (stacking) dipole interaction, in which the excitation is spatially delocalized across the two bases of the probe (Figure 8A) (29). For a nearly parallel arrangement of coupled transition dipoles, which is the expected situation for coupled $\pi \rightarrow \pi^*$ transitions within two stacked bases, the majority of the oscillator strength will go into the higher energy of the two exciton transitions (i.e. the e_+ state) (30). This effect is expected to diminish as the relative angle or distance between the two bases increases, consistent with our observations.

Interactions between neighboring 6-MI bases also decrease the fluorescence intensity per mole of 6-MI in ssDNA. Such apparent self-quenching within a dimer probe has been previously observed for 2-AP and PC dimer probes (1,4), and can be explained in the context of the exciton model. Immediately after the chromophore is excited, the majority of the excited state population is in the symmetric e_+ state. However, provided the excited chromophore can exchange energy with its local environment, it will—in accord with Kasha's rule—rapidly undergo internal conversion to the lowest excited electronic state (i.e., the e_- state) (31). Since the dipole matrix element that joins the ground and e_- state is small, relaxation to the ground state is likely dominated by

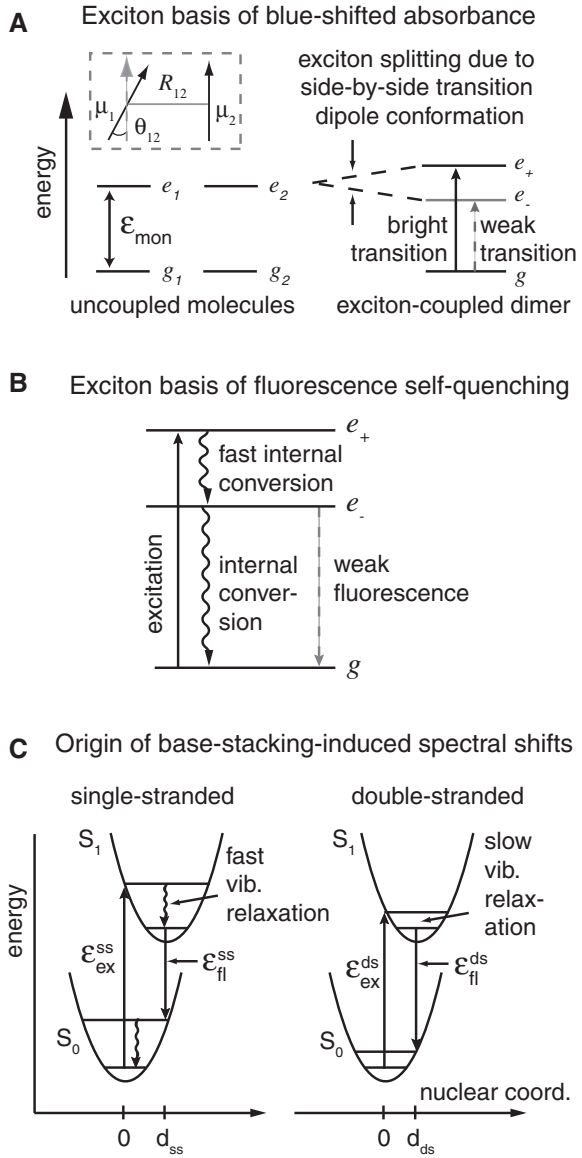

Figure 8. Energy level diagrams. (**A**) Two degenerate two-level molecules with transition energy ε_{mon}. The inset at the top shows the side-by-side configuration of two transition dipole moments, corresponding to the nearly parallel $\pi \rightarrow \pi^*$ transitions of two stacked bases. Interaction between transition dipoles results in an exciton-coupled dimer, with bright and dark excited states e_+ and e_-, respectively. The side-by-side (stacked) configuration results in a blue-shifted absorbance. (**B**) Fluorescence self-quenching of the dimer probe occurs due to rapid internal conversion of the initially excited population in the e_+ level to the lowest excited e. level. Because the e. state carries little oscillator strength, slow relaxation to the ground state occurs predominantly by internal conversion. (**C**) Duplex formation reduces electron-vibrational coupling between the probe and the aqueous solvent environment. The displacement parameter d is a measure of electron-vibrational coupling, described by the Franck-Condon principle. In our model, shielding of the chromophore from the aqueous environment in the duplex results in $d_{ds} < d_{ss}$, resulting in red-shifted absorbance and blue-shifted fluorescence.

non-radiative internal conversion processes (Figure 8B) (32), reflecting distinct decay pathways for the dimer probe that are not found for the monomer probe. This reasoning also helps to explain the inverse relationship between the fluorescence intensity and the intensity of the low energy CD spectra of these dimer probes (Figure 4).

Finally, comparison of 6-MI dimers probes located in either ssDNA or dsDNA strands revealed wavelength shifts in the UV absorption and fluorescence spectra of both the monomer and the dimer probes. A red shift was observed for the absorbance of 6-MI (Figure 2C and Table 1), reminiscent of the absorbance of 2-AP, which is also red-shifted in stacked duplex DNA (2). In contrast, the fluorescence emission of 6-MI shifted to *higher* energies relative to ssDNA for probes incorporated within dsDNA constructs. These wavelength shifts appear to depend on the sequence context of the probe for reasons that we do not yet understand. Nevertheless, we believe that to a first approximation these spectral shifts can be interpreted in terms of the polarizability of the local environment, as described by the Onsager theory of dielectrics and the Franck-Condon Principle (32).

According to the Franck-Condon Principle, electronic excitation of the probe occurs 'instantaneously', without a change in nuclear coordinates. This excitation corresponds to a vertical transition on a potential energy diagram (Figure 8C), which generally results in a vibrationally excited and polarized molecule on the S_1 excited-state manifold. Excess vibrational energy can dissipate through interactions with the solvent. Reorganization of the local probe environment that stabilizes the electronic excited state is referred to as electron-vibrational coupling, and determines the magnitude of the fluorescence Stokes shift. This effect is quantified by the distortion parameter *d*, which corresponds to the displacement of the minimum of the excited state potential energy surface relative to the ground state projected onto a relevant nuclear configuration coordinate.

Duplex formation enhances the base stacking of the 6-MI residues and shields the probe from direct contact with the aqueous solvent. In contrast, 6-MI probe bases within ssDNA constructs are exposed to the aqueous environment and the excited state can be readily stabilized through dielectric relaxation. Therefore the displacement parameter of the probe is expected to decrease within the duplex relative to probe bases in ssDNA ($d_{ds} < d_{ss}$), resulting in a red shift of the absorbance and a blue shift of the fluorescence signal (Figure 8C). Furthermore, because duplex formation corresponds to a reduction in electron-vibrational coupling, vibrational deactivation of the excited state of dsDNA is expected to be slow. As a result fluorescence from vibrationally 'hot' levels in the duplex is likely to be responsible for the observed dependence of the emission peak intensity on excitation wavelength (Supplementary Figure S1).

Effects of the 6-MI dimer on the stability and structure of DNA

The replacement of a GG dimer pair with two 6-MI residues decreases the T_m of duplex DNA by ~3.5°C (Figure 5 and Supplementary Figure S2). The 6-MI dimer probe melts cooperatively with the other DNA bp in the duplex, at least for our short DNA constructs,

indicating that the dimer probe does not significantly disrupt the local stability compared to the rest of the duplex DNA. Replacement of a G by a single 6-MI base (g) also somewhat destabilizes duplex DNA. T_m values (relative to the corresponding unmodified constructs) decrease by 0.4°C in 5′-GgA-, by 0.6°C in 5′-AgT- and 1.6°C in 5′-AgA- triplet sequences (33). These different T_m values probably arise from the slightly different stacking interactions of the 6-MI bases with their flanking bases in the duplex DNA, rather than reflecting H-bonding with the complementary C (which should be the same for all sequences). Likewise, the observation that two adjacent 6-MI bases destabilize dsDNA more than an isolated (single) probe base may reflect altered base stacking of the 6-MI residues with neighboring bases and/or with one another.

To further examine the effects of 6-MI on the dsDNA structure we used the small molecule solvent additive betaine (27,28), which is thought to bind preferentially in the major groove of B-form DNA at A•T bp. We found that the 6-MI dimer probe destabilized dsDNA to the same extent in the presence or absence of betaine. In contrast, for PC and 2-AP dimers probes in the same DNA sequence, betaine significantly increased or decreased, respectively, the stability of dsDNA relative to the unmodified constructs. These effects probably reflect differences in the chemical structures of these probes (Figure 5). Thus PC has an additional cyclic ring compared to cytosine, placing a methyl group in the major groove of B-form dsDNA that could contribute to an increased interaction with betaine. A hydrogen bond between the bases of the A•T bp is displaced from the major to the minor groove in the 2-AP•T bp, which might also alter the major-groove-binding environment for betaine. In contrast, the chemical modification associated with the 6-MI•C bp is further removed from the major groove of B-form DNA, which is consistent with our finding that betaine has no effect on the T_m changes associated with the presence of the 6-MI dimer probe. These results suggest that 6-MI may not significantly perturb the chemical or structural properties of the major groove, and also provide experimental support for the 6-MI•C base-pairing scheme proposed in Figure 1.

Finally we asked if the 6-MI dimer probe alters DNA conformations near the fork junction of P/T DNA, which can serve as a minimal substrate for DNA replication. 6-MI dimer probe residues in the first 2 bp of the dsDNA just upstream of the P/T junction are significantly unstacked at room temperature compared to probes in the 'interior' of duplex DNA (Figure 4). Very similar effects were observed at these positions using a 2-AP dimer as a conformational probe (4,5). Furthermore the decrease in the stability of the first bp downstream of the duplex junction seemed about the same as detected previously with 2-AP analog probes. Hence we conclude that the extent of DNA 'breathing' at the P/T junction may depend mostly on the presence of the ssDNA–dsDNA discontinuity itself, and is probably less dependent on local base-pair sequence.

Comparison of the 6-MI monomer and dimer probes as templates for DNA replication

Like G, a 6-MI dimer probe in the template strand preferentially codes for incorporation of dCTP relative to the other bases (3) (Supplementary Figure S3). However unlike G, 6-MI dimers probes in the ssDNA region of the template strand appear to inhibit primer *extension* (Figure 6). To better understand this difference between the templating activities and the extension activities of these probes, we have studied the replication of template DNA containing a single 6-MI residue.

Nucleotide addition opposite a single 6-MI templating base is as efficient as for G (Supplementary Figure S4) and (as expected) displays a strong preference for the complementary nucleotide dCTP (Figure 7C and Supplementary Table S2). However, once the nascent primer strand has been extended to form the first 6-MI•C bp with the template, further elongation is dramatically inhibited, although some full-length product is eventually observed in the presence of all four dNTPs (Figure 7B). These results suggest that inhibition of replication synthesis as a consequence of the presence of the 6-MI dimer probe primarily reflects a slowing or stalling of primer extension *after* incorporation by the DNAP of the first residue coded by the first 6-MI templating base encountered.

A complex between KF DNAP and a P/T DNA construct with a single 6-MI•C bp at the 3′ primer terminus (6-MI dimer in the template strand) has been previously studied. The 6-MI•C bp does not appear to be treated by the DNAP as a terminal mismatch, since the relative distribution of the 3′-end of the primer strand between the *pol*- and the *exo*- site of the polymerase is the same as observed for the binary complex with a fully base-paired P/T junction [see Figure 4C in (3)]. However, binding of KF DNAP to a P/T DNA construct carrying a 3′-terminal 6-MI•C bp is very slow compared to the rate of association to an unmodified construct, suggesting that reassociation would be difficult if the stalled complex dissociated. Alternatively 6-MI dimers in duplex DNA contiguous to the P/T junction also decrease the replication efficiency of KF DNAP (Figure 6). These results suggest that the 6-MI dimer probe might perturb the interactions between the polymerase and the duplex region of the P/T DNA that are important for binding and/or translocation during primer extension.

Summary

We conclude that electronic interactions between the bases of the 6-MI dimer probe can provide spectral (and thus structural) information that is not available using single 6-MI probes. The low energy CD spectrum located at ~350 nm is particularly informative and in favorable circumstances can be associated with specific DNA conformations. Unlike 2-AP, no 'spill-over' signal from proteins or canonical DNA bases is observed in the CD spectra of 6-MI. PC base analogs share this advantage of a well-separated transition at 350 nm, but both the absorbance and the fluorescence quantum yields for PC are smaller than for 6-MI. Thus the 6-MI dimer can serve as

a useful probe for monitoring the conformations of adjacent GG residues in DNA and RNA.

SUPPLEMENTARY DATA

Supplementary Data are available at NAR Online: Supplementary Tables S1–S2 and Supplementary Figures S1–S5.

ACKNOWLEDGEMENTS

The authors thank Walt Baase and members of our laboratories for helpful advice and discussions. NPJ thanks Serge Mazeres of the 'Toulouse Réseau Imagerie' core IPBS facility (Genotoul, Toulouse, France) for expert technical assistance. P.H.vH is an American Cancer Society Research Professor of Chemistry.

FUNDING

National Institutes of Health grant (GM-15792 to P.H.vH.); Agence Nationale de la Recherche grant (Mobigen to N.P.J.); Centre Nationale de la Recherce Scientifique salary support for N.P.J.; from the Institut National de la Santé et de la Recherche Medicale salary support for G.V.; National Science Foundation Chemistry of Life Processes Program (CHE-1105272) and the Office of Naval Research (Grant N00014-11-1-0193 to A.H.M). Funding for open access charge: National Institutes of Health.

Conflict of interest statement. None declared.

REFERENCES

1. Johnson,N.P., Baase,W.A. and von Hippel,P.H. (2005) Investigating local conformations of double-stranded DNA by low-energy circular dichroism of pyrrolo-cytosine. *Proc. Natl Acad. Sci. USA*, **102**, 7169–7173.
2. Johnson,N.P., Baase,W.A. and Von Hippel,P.H. (2004) Low-energy circular dichroism of 2-aminopurine dinucleotide as a probe of local conformation of DNA and RNA. *Proc. Natl Acad. Sci. USA*, **101**, 3426–3431.
3. Datta,K., Johnson,N.P. and von Hippel,P.H. (2010) DNA conformational changes at the primer-template junction regulate the fidelity of replication by DNA polymerase. *Proc. Natl Acad. Sci. USA*, **107**, 17980–17985.
4. Jose,D., Datta,K., Johnson,N.P. and von Hippel,P.H. (2009) Spectroscopic studies of position-specific DNA ''breathing'' fluctuations at replication forks and primer-template junctions. *Proc. Natl Acad. Sci. USA*, **106**, 4231–4236.
5. Datta,K., Johnson,N.P., LiCata,V.J. and von Hippel,P.H. (2009) Local conformations and competitive binding affinities of single- and double-stranded primer-template DNA at the polymerization and editing active sites of DNA polymerases. *J. Biol. Chem.*, **284**, 17180–17193.
6. Datta,K. and von Hippel,P.H. (2008) Direct spectroscopic study of reconstituted transcription complexes reveals that intrinsic termination is driven primarily by thermodynamic destabilization of the nucleic acid framework. *J. Biol. Chem.*, **283**, 3537–3549.
7. Datta,K., Johnson,N.P. and von Hippel,P.H. (2006) Mapping the conformation of the nucleic acid framework of the T7 RNA polymerase elongation complex in solution using low-energy CD and fluorescence spectroscopy. *J. Mol. Biol.*, **360**, 800–813.
8. Johnson,N.P., Baase,W.A. and von Hippel,P.H. (2005) Low energy CD of RNA hairpin unveils a loop conformation required for lambdaN antitermination activity. *J. Biol. Chem.*, **280**, 32177–32183.
9. Repges,R., Beuck,C., Weinhold,E., Raabe,G. and Fleischhauer,J. (2008) 6-Thioguanine in DNA as CD-spectroscopic probe to study local structural changes upon protein binding. *Chirality*, **20**, 978–984.
10. Baase,W.A., Jose,D., Ponedel,B.C., von Hippel,P.H. and Johnson,N.P. (2009) DNA models of trinucleotide frameshift deletions: the formation of loops and bulges at the primer-template junction. *Nucleic Acids Res.*, **37**, 1682–1689.
11. Hawkins,M.E. (2001) Fluorescent pteridine nucleoside analogs: a window on DNA interactions. *Cell Biochem. Biophys.*, **34**, 257–281.
12. Hawkins,M.E., Pfleiderer,W., Balis,F.M., Porter,D. and Knutson,J.R. (1997) Fluorescence properties of pteridine nucleoside analogs as monomers and incorporated into oligonucleotides. *Anal. Biochem.*, **244**, 86–95.
13. Myers,J.C., Moore,S.A. and Shamoo,Y. (2003) Structure-based incorporation of 6-methyl-8-(2-deoxy-beta-ribofuranosyl)isoxanthopteridine into the human telomeric repeat DNA as a probe for UP1 binding and destabilization of G-tetrad structures. *J. Biol. Chem.*, **278**, 42300–42306.
14. Poulin,K.W., Smirnov,A.V., Hawkins,M.E., Balis,F.M. and Knutson,J.R. (2009) Conformational heterogeneity and Quasi-static self-quenching in DNA containing a fluorescent guanine analogue, 3MI or 6MI. *Biochemistry*, **48**, 8861–8868.
15. Parsons,J. and Hermann,T. (2007) Conformational flexibility of ribosomal decoding site RNA monitored by fluorescent pteridine base analogues. *Tetrahedron*, **63**, 3548–3552.
16. Johnson,S.J., Taylor,J.S. and Beese,L.S. (2003) Processive DNA synthesis observed in a polymerase crystal suggests a mechanism for the prevention of frameshift mutations. *Proc. Natl Acad. Sci. USA*, **100**, 3895–3900.
17. Kiefer,J.R., Mao,C., Braman,J.C. and Beese,L.S. (1998) Visualizing DNA replication in a catalytically active Bacillus DNA polymerase crystal. *Nature*, **391**, 304–307.
18. Li,Y., Korolev,S. and Waksman,G. (1998) Crystal structures of open and closed forms of binary and ternary complexes of the large fragment of Thermus aquaticus DNA polymerase I: structural basis for nucleotide incorporation. *EMBO J.*, **17**, 7514–7525.
19. Joyce,C.M., Potapova,O., Delucia,A.M., Huang,X., Basu,V.P. and Grindley,N.D. (2008) Fingers-closing and other rapid conformational changes in DNA polymerase I (Klenow fragment) and their role in nucleotide selectivity. *Biochemistry*, **47**, 6103–6116.
20. Purohit,V., Grindley,N.D. and Joyce,C.M. (2003) Use of 2-aminopurine fluorescence to examine conformational changes during nucleotide incorporation by DNA polymerase I (Klenow fragment). *Biochemistry*, **42**, 10200–10211.
21. Santoso,Y., Joyce,C.M., Potapova,O., Le Reste,L., Hohlbein,J., Torella,J.P., Grindley,N.D. and Kapanidis,A.N. (2010) Conformational transitions in DNA polymerase I revealed by single-molecule FRET. *Proc. Natl Acad. Sci. USA*, **107**, 715–720.
22. Tsai,Y.C. and Johnson,K.A. (2006) A new paradigm for DNA polymerase specificity. *Biochemistry*, **45**, 9675–9687.
23. Ramsay,G.D. and Eftink,M.R. (1994) Analysis of multidimensional spectroscopic data to monitor unfolding of proteins. *Methods Enzymol.*, **240**, 615–645.
24. Joyce,C.M. and Derbyshire,V. (1995) Purification of Escherichia coli DNA polymerase I and Klenow fragment. *Methods Enzymol.*, **262**, 3–13.
25. Doose,S., Neuweiler,H. and Sauer,M. (2009) Fluorescence quenching by photoinduced electron transfer: a reporter for conformational dynamics of macromolecules. *Chemphyschem*, **10**, 1389–1398.
26. Torimura,M., Kurata,S., Yamada,K., Yokomaku,T., Kamagata,Y., Kanagawa,T. and Kurane,R. (2001) Fluorescence-quenching phenomenon by photoinduced electron transfer between a fluorescent dye and a nucleotide base. *Anal. Sci.*, **17**, 155–160.

27. Hong,J., Capp,M.W., Anderson,C.F., Saecker,R.M., Felitsky,D.J., Anderson,M.W. and Record,M.T. Jr (2004) Preferential interactions of glycine betaine and of urea with DNA: implications for DNA hydration and for effects of these solutes on DNA stability. *Biochemistry*, **43**, 14744–14758.
28. Rees,W.A., Yager,T.D., Korte,J. and von Hippel,P.H. (1993) Betaine can eliminate the base pair composition dependence of DNA melting. *Biochemistry*, **32**, 137–144.
29. Cantor,C.R. and Schimmel,P.R. (1980) (II). In Freeman,W.H. (ed.), *Techniques for the Study of Biological Structure and Function*. Biophysical Chemistry, New York.
30. Kasha,M., Rawls,H.R. and Ashraf El-Bayoumi,M. (1965) The exciton model in molecular spectroscopy. *Pure Appl. Chem.*, **11**, 371–392.
31. Kasha,M. (1950) Characterization of electronic transitions in complex molecules. *Disc. Faraday. Soc.*, **9**, 14–19.
32. Birks,J.B. (1970) *Photophysics of Aromatic Molecules*. Wiley-Interscience, London.
33. Hawkins,M.E., Pfleiderer,W., Jungmann,O. and Balis,F.M. (2001) Synthesis and fluorescence characterization of pteridine adenosine nucleoside analogs for DNA incorporation. *Anal. Biochem.*, **298**, 231–240.